Author postprint version of the Chapter 16 of "Advanced Instrument Engineering: Measurement, Calibration, and Design", pages 208-222, IGI Global (2013) Edited by Aymé Lay-Ekuakille

AC magnetic measurements on superconductors : design of a device for magneto-thermal measurements

Philippe Laurent, Jean-François Fagnard and Philippe Vanderbemden
SUPRATECS and Department of Electrical Engineering and Computer Science B28, University of Liège, Sart-Tilman, B-4000 Liège, Belgium

ABSTRACT

This work describes the design and realisation of an apparatus to measure simultaneously the AC magnetic properties and the temperature distribution on the top surface of bulk superconducting samples (up to 32 mm in diameter) in cryogenic conditions (temperature range 78-120 K). First we describe the experimental set-up used for simultaneous thermal and magnetic characterization of the sample. Next we describe the practical considerations required for generating the large AC magnetic fields, possibly in the presence of DC fields. In the third section we present a custom-made high speed data acquisition system for replacing the laboratory devices (DC voltmeter and AC lock-in amplifiers) when both temperature and magnetic data need to be recorded at high a sampling rate. The performances and limitations of the system are discussed.

Keywords: superconductors, temperature measurement, magnetic measurements, AC susceptibility.

1. INTRODUCTION

Superconductors are materials that exhibit zero resistance under a given temperature, called critical temperature T_c. In addition to carrying lossless currents, superconductors are also characterised by several unusual and attractive magnetic properties (e.g. levitation, magnetic shielding, ...) that are relevant for a number of engineering applications (Campbell, 1997). The measurement of their AC magnetic properties as a function of temperature represents a well-established and powerful tool for studying their performances (Goldfarb, 1991). The AC susceptibility χ of a superconductor can be expressed as $\chi = \chi' - j\chi''$, where the real part (χ') represents flux exclusion due to induced shielding currents in the superconductor and the imaginary part (χ'') is proportional to the magnetic losses (Gömöry, 1997). These losses may give rise to a significant temperature increase and a degradation of the superconducting properties (Yamaguchi, 2006). It is therefore desirable to measure simultaneously the AC magnetic properties and the corresponding self-heating (Fujishiro, 2006). In a previous work (Laurent, 2008), we have described an original AC susceptometer (i.e. a device for measuring AC susceptibility) suitable for measuring precisely the AC magnetic properties of large (up to 32 mm diameter) superconducting samples as a function of temperature, which is considerably larger than the size of the samples that can be accommodated in commercial devices (typically 10 mm diameter). In the present work, we describe how such an AC

susceptometer can be upgraded in view of recording simultaneously the AC magnetic properties of the superconductor and the temperature at several locations on the sample surface.

This paper is organized as follows. In the first section we describe the practical considerations required for achieving simultaneous measurements of magnetic properties and of the temperature distribution along the surface of a bulk superconducting sample subjected to an AC magnetic field. In particular we describe detail the experimental precautions to be taken for precise temperature measurements in the presence of magnetic fields in the audio frequency range. The second section is devoted to the generation of magnetic fields. The performances and limitations of the magnet are measured, reported and discussed. In the third section we describe the signal conditioning (amplification and filtering) and the subsequent numerical treatment of the digitized data in order to extract precisely low DC and AC signals in a noisy environment.

2. INSTRUMENTATION OF THE SUPERCONDUCTING SAMPLE

Basically, a susceptometer consists of a magnetizing (primary) coil and two pick-up (secondary) coils wound electrically in series opposition (Nikolo, 1995). The electro-motive force (emf) induced across ideal pick-up coils (i.e. wound with the same number of turns and in identical geometries) is zero in the absence of a sample. Inserting a magnetic sample centred in one of the secondary coils results in the generation of a non-zero signal that is directly proportional to the AC magnetic susceptibility.

In the experiment described here, the classical set-up is extended to measure simultaneously (i) the temperature against the top surface of the superconducting sample and (ii) the magnetic flux density against the bottom surface of the sample, as shown in figure 1. In the following we describe the temperature sensors and the magnetic sensors.

2.1 TEMPERATURE SENSORS

The temperature sensors are used to give information on the time-evolution of the temperature distribution over the top surface of the sample (i.e. along the radius if an axial symmetry is assumed) during the application of the AC magnetic field. The temperature sensors attached to the superconductor must therefore be characterized by a small response time. In this work, thermocouples are chosen in view of their tiny size (< 1mm) and response times much smaller than 1 s. We use Type E thermocouples, i.e. chromel (90% Ni - 10% Cr) - constantan (55% Ni - 45% Cu). Type E thermocouples are characterized by a high sensitivity (68 µV/K at room temperature, ~ 28 µV/K in the 77-92 K interval) and are well suited to cryogenic use. In addition, they are non-magnetic and therefore can be used under large magnetic fields. In our set-up, thermocouples were fabricated using of the thinnest possible diameter wires (50 µm). This gives the following advantages. First, the response time is minimal. Second, thin thermocouples are easier to attach on the sample surface thanks to good mechanical flexibility. Third, the large thermal resistance (inversely proportional to the wire cross-section) allows one to minimize the thermal losses by conduction through the wires. In the case of our wires, the thermal resistance is evaluated at ~ 10^6 K/W at 77 K, using thermal conductivities given in (Sundqvist, 1992).

The two ends of a thermocouple are usually called “hot junction” (or “measurement junction”) and “cold junction” (or “reference junction”). It is important to note that thermocouples always measure a temperature difference, not an absolute temperature. Therefore the temperature of the reference junction has to be known precisely. In our experiment, 3 thermocouples are used and the 3x2 reference junctions are thermalized on an alumina plate whose temperature is recorded by a Pt-100 platinum resistance thermometer thermally anchored to it (figure 2). A second alumina plate, slightly hollowed by a diamond millstone, is placed on the top of the previous plate to encapsulate cold junctions and the resistor together. Alumina exhibits a good thermal conductivity as well as a low electrical conductivity. This latter property is required to avoid the occurrence of eddy currents which would possibly modify the characteristics of the AC magnetizing field. Furthermore, alumina (ceramic Al_2O_3) is much cheaper than sapphire (crystalline Al_2O_3), which is used commonly as an electrically non-conducting heat sink.

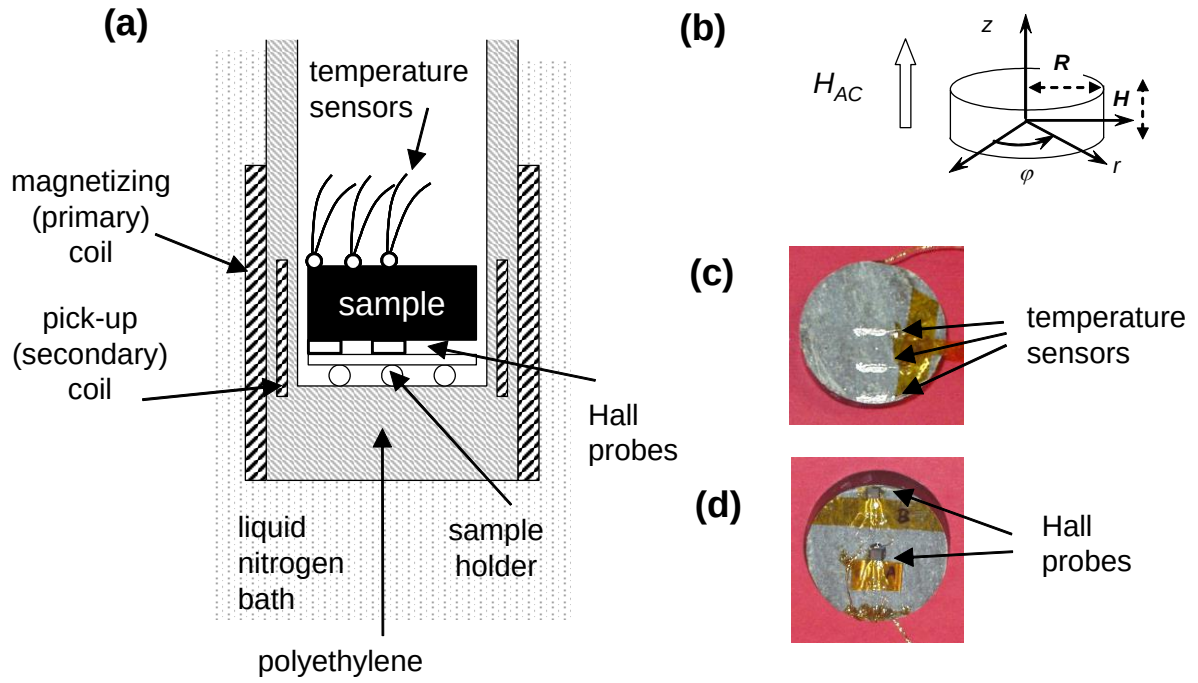

Figure 1. (a) Schematic illustration of the bottom of the experimental chamber of the AC susceptometer used for self-heating measurements. (b) Schematic illustration of the superconducting sample. (c) Top view of the sample top surface, showing three equally-spaced thermocouples located along the radius. Thin cigarette paper is placed between the superconductor and the sensors to avoid electrical shortcut between hot junctions. To increase the mechanical resistance for handling, 50 µm thin wires of thermocouples are sandwiched between two Kapton® tapes. (d) View of the sample bottom surface showing the location of the two Hall probes; one (A) at the sample centre and the second (B) close to the sample edge.

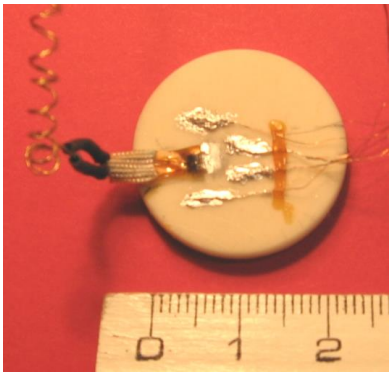

Figure 2. Reference junction of thermalized the alumina plate whose temperature is monitored by a Pt-100 platinum resistance thermometer.

In our experimental system, all constantan legs of the thermocouples are connected together and thermalized on the alumina plate. The thermal anchorage of junctions of thermocouples is realized with silver paint which acts both as soldering and as a thermally conductive paste as well (the thermal conductivity of silver is 478 W/m.K at the liquid nitrogen temperature 77.4 K). Since constantan legs are at the same voltage, the three hot junctions should be insulated from each other. In practice electrical insulation is achieved using thin cigarette paper glued on the sample top surface with GE 7031 varnish. The three measurement junctions are located on the sample at different radii to check the temperature distribution: one in the centre ($r = 0$), on near the edge ($r = R$), and the last one in between ($r = R/2$) (see figure 1(c)).

Note that due to large heat capacity of alumina, the temperature of the cold junctions (T_{ref}) of the thermocouples does not vary much during a complete measurement run. This temperature is very close to the superconductor temperature (T_s). In practice, the temperature difference between the hot and the cold junctions was found to never exceed ~ 10 K and heat losses by thermal conduction (Q_{cond}) through the thermocouple legs are found to be negligible with respect to the typical heat transfer occurring between the sample and the experimental chamber walls.

The typical voltage appearing across a thermocouple is usually small (< 1 mV) and requires a lot of care to be taken. An important issue is the accurate measurement of a small DC voltage under AC magnetic field of possibly high amplitudes; an unwanted significant AC voltage is likely to be induced by inductive pick-up. To reduce the amplitude of this voltage as much as possible, thermocouples legs are twisted all along their length to minimize the loop size. Despite of a careful leg twisting, a remaining AC voltage coming from the external applied field, but also from the power line (50 Hz) has to be removed. When the temperature increase is relatively slow (i.e. at “relatively” small AC field amplitudes), each thermocouple voltage is read with a high sensitivity voltmeter. The integration time of the voltmeter is thus set as an integer multiple of *both* the power line cycle (PLC, 20 ms) and the period of the applied magnetic field. In so doing, error voltages coming from the power line and/or from the applied field are averaged out to approximately zero. When the temperature increase is fast (i.e. at “relatively” large AC field amplitudes), the GPIB connections between the devices recording the magnetic and temperature data are usually found to be too slow. Therefore the thermocouple voltages are amplified and recorded using a high speed data acquisition card, as will be described in the last section of this paper. In this case, the averaging is done numerically after the data acquisition.

Another issue is that the number of electrical connections between the outputs of the thermocouple and the measuring device must be kept minimal. Indeed, thermoelectric voltages appearing at the connections between dissimilar materials are the most common source of error in low-level DC measurements. Thus, attaching copper wire to the pins of the electrical feedthrough with tin-lead solder (Sn/Pb) must be realised with great care to avoid voltages coming from unwanted "thermocouple" Sn/Pb-Cu. The typical thermoelectric voltage for a Cu and Sn/Pb connection is approximatively 5 µV/K. In order to cancel possible thermoelectric voltage generated between the soldering agent and copper, several turns of copper wire are wrapped around the pin before brazing with solder. This procedure ensures that the set "pin+solder+wire" can be considered as isotherm.

2.2 MAGNETIC SENSORS

When the superconductor is subjected to an AC magnetic field, its properties are measured by two ways. First, the global AC magnetic flux threading the whole cross-section of the sample is determined from the electromotive force (emf) induced across the pick-up coils of the AC susceptometer. Second, in order to obtain additional information about the magnetic flux density distribution, two AHP-H3Z Arepoc® Hall probes are fixed on the bottom surface of the pellet, one in the sample centre and the other at ~ 1 mm from the edge, as shown in figure 1(d). Note that Hall probes (attached to the bottom surface) and the thermocouples (attached to the top surface) are purposefully placed on different surfaces to avoid any influence of the Hall probes on the temperature measurement. The Hall probes have a typical active area of 1 mm^2 and a size of 2.3 x 2.8 x 1.0 mm^3. Here again, cigarette paper is glued to the surface with GE varnish to avoid electrical shortcut between the Hall probe leads.

To connect the Hall probe leads to the hermetic seal feedthrough of the vacuum chamber of our cryogenic susceptometer, 100 µm diameter manganin wires are used. Manganin is characterised by a sufficiently high electrical conductivity while exhibiting a high thermal resistivity. In addition, manganin wires have better mechanical properties than copper wires of the same dimensions. Wires are twisted all along their length to reduce as much as possible the size of eventual loops.

Some care is required for the calibration process of the Hall probes. A nominal control current I = 10 mA is recommended in the Hall probe datasheet. Using such a current, however, the total dissipated power for the two sensors (each of them having a resistance R ~ 400 Ω at 77.4 K) lies around 80 mW. This is large enough, in semi-adiabatic conditions at cryogenic temperature, to induce a significant temperature increase read by thermocouples. For this reason, the control current of Hall probes is taken to be equal to 1 mA so that the Joule effect is reduced by a factor 100 whereas the Hall voltage is only reduced by a factor 10. For a given control current I and magnetic flux density B, the Hall voltage is usually a function of the Hall sensor temperature. Since the sensitivity at 77.4 K is ~ 1.5 times higher than the sensitivity at room temperature, both Hall sensors are calibrated at 77.4 K. Since the Hall probes are to be used for measuring both AC and DC magnetic fields, two calibration procedures are carried out.

The DC calibration is performed in a DC magnetic field up to $\mu_0 H_{DC}$ ~ 500 mT and the DC voltage is recorded with a high-sensitivity DC voltmeter. The AC calibration is carried out in an AC field of smaller amplitude (~ 1 mT) and the AC Hall voltage is measured using a lock-

in amplifier. The AC method, despite a smaller magnetic field range, has two advantages over the DC calibration: (i) DC thermoelectric voltages do not affect the measurements and (ii) the frequency dependence of the out-of-phase component gives information on the unwanted inductive pick-up. We have checked experimentally that increasing the frequency of the AC field at constant amplitude has no effect of the AC amplitude of the Hall probe voltage; this suggests that the wire twisting is efficient.

Both DC and AC procedures should theoretically give the same sensitivity. Carring out two calibrations, however, allows one to identify the sources of measurement errors and minimize them. The two calibration methods provide very similar sensitivity for each probe respectively. However, a slight difference of sensitivity between the two probes is observed (109.5 mV/T against 116.5 mV/T in AC mode at 77.4 K with 10% of the nominal current).

The last point to be mentioned in this section is that Hall probes are very fragile and may be destroyed by a current or voltage overshoot. An efficient way to protect these probes is to place a capacitor (typically 330 nF) in parallel with the voltage leads in order to deviate a large part of any unwanted transient current. In order to avoid voltages exceeding the maximum input voltage, two Zener diodes (V_Z = 12 V), placed in series opposition, are placed in parallel with this capacitor.

3. GENERATION OF SUPERIMPOSED AC AND DC MAGNETIC FIELDS

In this section, we study the experimental issues associated with the generation of the largest AC magnetic fields with our system, and how they can be overcome. We also investigate the practical considerations for superimposing a DC field to the AC field. We restrict ourselves to the practical experimental conditions:

- Both AC and DC coils are made of copper wire; this differs from some other experimental set-ups involving a superconducting magnet cooled with liquid helium. In our system no liquid helium is used but the copper coils are cooled down to the liquid nitrogen temperature (77.4 K) to decrease their electrical resistance by a factor ~1/8 with respect to the room temperature resistance.

- No ferromagnetic circuit is used (e.g. laminated iron or ferrite) in order to make sure that no spurious phase-lag or signal distortion is induced.

In our system, two concentric air coils are used.

- The inner coil is fed with AC current and generates the AC magnetic field. The coil can sustain ~ 6A at 77.4 K and its B/I ratio is equal to 24 mT/A.

- The outer coil is made of copper tape of large cross-section (2 x 4 mm^2) and is fed with DC current to generate the DC magnetic field. The coil can sustain ~ 100A at 77.4 K and its B/I ratio is equal to 5.4 mT/A. The AC coil can be inserted easily in the DC coil.

Taking the characteristics mentioned above, one would think intuitively that an AC field of 144 (= 6 × 24) mT can be superimposed onto a DC field of 540 (= 100 × 5.4) mT with the two coils. The real maximum AC and DC field values, however, are substantially smaller because of practical limitations mentioned below.

3.1 GENERATION OF LARGE AC MAGNETIC FIELDS

One of the main problems in generating large AC magnetic field is linked to the large voltage drop V_{AC} across the magnetising coil (resistance R, inductance L). In this work, the frequency range studied is limited to the 50 – 120 Hz interval. In this frequency range, the magnetizing coil can be fed with a 6A [RMS] current. As far as temperature measurements are concerned, however, the power dissipated by Joule effect in the copper windings should be small enough in order not to influence the sample temperature. In our system, we have determined that the maximum current in the magnetizing coil should be kept below 2.5 A [RMS] in order to make sure that the sample temperature is independent of the magnetizing current. This criterion leads to a maximum field of 60 mT [RMS] with our system. Such a value is well in excess of those attainable with commercial AC susceptometers (e.g. typically 1.7 mT in the Quantum Design PPMS or 2 mT in the Lake Shore AC susceptometer).

It is of interest to compare the performance of our magnet to those of the home-made systems described in the literature, see e.g. (Vanderbemden, 1998). A few of them generate AC fields of larger amplitudes, but none of them matches the requirements of our application. In ref (Gömöry, 1994), for example, magnetic fields up to 100 mT can be generated but within a volume which is significantly smaller than our typical sample size. In ref. (Zushi, 2004) magnetic fields are applied up to 100 mT in the range 7-245 Hz but at constant temperature (77.4 K). Recently, a race-track coil system was described (Trojanowski, 2007) for generating large AC magnetic fields with excellent field-uniformity over a 80 mm length, but the system is optimized for long superconducting tapes whose size differs from cylindrical bulk superconductors that are to be characterized in this work. Finally, an iron-core electromagnet was developed in our laboratory to generate AC magnetic fields exceeding 130 mT (Lousberg, 2009) but this maximum field can be obtained in a relatively narrow frequency window (25-30 Hz).

In order to prevent high amplitude AC magnetic fields from reaching human body, the whole experimental set-up is placed in a large iron enclosure acting as a magnetic shield. Magnetizing coils are located enough far away from box walls so that they do not affect the offset of the pick-up coils. The magnetic flux density measured at 1 meter from the box is ~ 10 μT at 50 Hz, i.e. 10 times less than the 100 μT threshold value recommended by the International Commission on Non-Ionizing Radiation Protection (ICNIRP) for the exposure of general public to time-varying magnetic fields at the same frequency.

A HP 8904A function generator followed by a CROWN XTi 2 kW audio amplifier is used to generate the AC current in the magnetizing (primary) coils of the susceptometer. Since the audio amplifier output is symmetrical with respect to the ground voltage, a decoupling transformer is inserted between the audio amplifier and the load. The load consists of the two magnetizing coils of the susceptometer, placed in series with a reference shunt resistor R_{ref} (~ 0.5 Ω) able to sustain large currents (figure 3). The two magnetizing coils are immersed in a liquid nitrogen bath, so that their resistance is negligible with respect to their reactive impedance. A bank of capacitors placed in series with the magnetizing coils in order to compensate the inductive load and lower the total impedance. The value of the total capacitance is set so that the working frequency matches the resonance frequency of the LC dipole.

Interestingly we have observed the following phenomenon : a large variation of the magnetising current is observed when the material becomes superconducting, i.e. when the temperature is below the critical temperature Tc. This effect is caused by a modification of the magnetizing coil inductance by the superconductor. On lowering the temperature, the transition from the normal to the superconducting state (flux exclusion) reduces the inductance of the magnetizing coil by approx. 8%. This inductance reduction has a drastic effect on the total impedance load since the resonance condition no longer holds. The observable variation of the magnetizing current (> 10 %) directly affects the magnetic field amplitude in the vicinity of T_c. In order to minimize the variation of the magnetizing current (and of the applied magnetic field), a damping resistor of sufficiently high resistance is inserted in series with the load; in our case a 30 Ω resistor was found to give very satisfactory results.

3.2 GENERATION OF DC MAGNETIC FIELDS SUPERIMPOSED TO THE AC FIELD

Now we turn to the experimental issues associated with the coil generating the DC magnetic field superimposed on the AC field. Due to the presence of the AC coil (inductance L_{1s}) within the DC coil, the DC coil (inductance L_{DC}) picks up a part of the AC magnetic flux, through the mutual inductance M_{AD}. This results in an induced AC voltage across the DC coil; the frequency of this voltage is that of the variable applied field. An AC current is therefore induced in the DC circuitry; this current modifies the characteristics of the AC magnetic field (amplitude and phase) at the sample location. An efficient way to reduce this effect and to protect the DC power supply from damage is to insert a LC resonant filter placed in series with the DC coil, as schematically illustrated in figure 3.

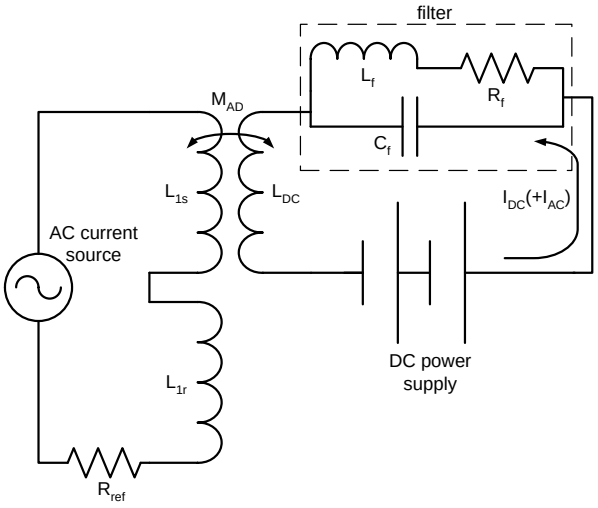

Figure 3. Schematic illustration on an LC resonant filter inserted in the DC circuitry in order to increase the AC impedance of the DC loop. The filter reduces the induced AC current I_{AC} passing through the DC coil; C_f is the capacitance of the filter capacitor and R_f and L_f denote the resistance and the inductance of the filter coil.

The filter capacitor has a capacitance C_f. The filter coil has an inductance L_f and a resistance R_f, its quality factor is given by $Q = \omega L_f / R_f$. The total impedance of the LC filter Z_f has a maximum value at the resonance frequency. For a low-loss coil ($Q >> 1$), the impedance Z_f is

given by $Z_f \approx R_f Q^2$. In order to maximize Z_f and therefore the LC filter efficiency, R_f must be as small as possible. In our case, the filter coil is made of thick copper wire (diameter = 4 mm) and the resistance R_f is reduced by a factor ~ 8 with respect to the room temperature value by cooling the whole filter coil in a liquid nitrogen bath.

The procedure to minimize the AC current in the DC loop is as follows. First, the working frequency f is chosen and the value of the capacity C_f is determined to match the resonance frequency coarsely, i.e. $f \approx f_0$. The frequency of the applied magnetic field is then fine tuned in order to minimize the offset voltage (read at the lock-in amplifier) across the two pick-up coils in series-opposition, the sample being in the normal (non-superconducting) state, i.e. just above its superconducting transition temperature T_c.

The maximum value of the DC field H_{DC} depends on several factors: (i) the maximum current that can sustain the coils in the DC circuit (i.e. both the DC magnet coil and the filter coil), (ii) the maximum current that can be delivered by the power supply, and (iii) the maximum power that can be tolerated in the coils without thermal runaway in the liquid nitrogen bath over the duration of the experiment (typically several hours).

In our experimental system, both coils can sustain ~ 100 A for a short period of time. The circuit is powered by a HP 6031A DC power supply (120 A, 20 V, 1000 W). Bolt connections between the coils and the power supply are used to minimize the total resistance of the DC loop; at 77.4 K, a value of 0.185 Ω is obtained. Great care is needed to reach such a low value: electrical contact surfaces are cleared from oxidation, connections are bolted and the length of the current leads is minimized. Given the characteristics of the power supply, such a resistance limits the current to ~ 73 A. In practice however, the strongest limitation of the maximum DC current arises from the risk of thermal runaway in the liquid nitrogen bath because of the power dissipated by Joule effect in the coils. We can analyze theoretically the maximum current that can be tolerated in the liquid nitrogen-cooled copper windings in the following manner. First we express the temperature dependence of the total resistance $R(T)$ of the two coils (i.e. the DC coil and the filter coil):

$$R(T) = R_0 \cdot (1 + \alpha \cdot (T - T_0)) \tag{1}$$

where, in our case, R_0 = 0.185 Ω at T_0 = 77.4 K and α denotes the temperature coefficient of the resistivity (α = $6.8.10^{-3}$ K^{-1} for copper). Under a current I, the heat flux Q_{gen} generated by Joule effect reads

$$Q_{gen} = R(T) I^2 = R_0 I^2 (1 + \alpha \cdot (T - T_0)) \tag{2}$$

The heating of the copper tape is balanced by the cooling provided by liquid nitrogen. The heat flux rate exchanged with the liquid nitrogen at its boiling temperature is given by

$$Q_{out} = A \cdot h_{LN2}(T_{wall}) \cdot (T_{wall} - T_{env}) \tag{3}$$

where A is the area of the exchange surface between the copper and the cryogenic fluid (units: m^2), T_{wall} is the temperature of the copper widing directly in contact with the liquid nitrogen at temperature T_{env} (units: K) and h_{LN2} (units: W/(m^2.K)) is the convective heat transfer coefficient. This convective heat transfer coefficient depends strongly on the temperature T_{wall}

because of a succession of different pool boiling regimes (Brentari, 1958) and reaches a maximum value of around 11000 W/(m².K) for a temperature ≈ 90 K. Consequently, the $Q_{out}(T)$ curve displays also a maximum at some temperature $T_m \approx 92$ K. Two regimes can therefore be observed : (i) for $T < T_m$, $dQ_{out}/dT > 0$; this corresponds to the stable part for which the heat flux leaving the hot wall increases when its temperature increases and (ii) for $T > T_m$, $dQ_{out}/dT < 0$, i.e. the unstable part for which Q_{out} decreases when the temperature of the wall increases.

From this result, it can be concluded that the current I in the coils should always be such that the winding temperature never exceeds $T_m \sim 92$ K. The winding temperature can be estimated experimentally through a measurement of its electrical resistance. In our experimental system, the maximum DC current supply in the DC loop was limited to 30 A, which corresponds to a DC magnetic field $\mu_0 H_{DC} = 162$ mT. Note that this value corresponds to the maximum magnetic field that can be applied simultaneously with the AC field. If the DC field is to be applied without superimposed AC field (e.g. for magnetizing the superconducting sample), the filter coil can be removed, the restrictions mentioned above no longer apply and the coil can be used to generate a DC field of ~ 500 mT.

4. MAGNETIC AND TEMPERATURE DATA ACQUISITION

In this section, we describe the data acquisition system required to record the time-dependence of the sample temperature as well as magnetic quantities when the superconductor is subjected to large AC magnetic fields (typically > 20 mT). Under such conditions, the magnetic losses are significant, and the temperature of the sample rises rather quickly (e.g. 5 K/min). As a consequence, data acquisition with traditional laboratory measuring devices (lock-in amplifier for magnetic signals, DC voltmeters for thermocouples) that are computer-controlled with GPIB is found to be much too slow to record precisely the temperature during the application of the AC field. We show here below how the devices can be conveniently replaced by a high-speed acquisition card.

In our application, we use a PCI 6221 DAQ board from National Instruments. The board can record up to 8 channels simultaneously with a high sampling rate (up to 250 kS/s); in practice the sample rate is fixed at 1 kS/s. The resolution of the analog-to-digital converter (ADC) is 16 bits. Using the lower sensitivity range (± 20 mV), this corresponds to a resolution of ~ 6 μV. The low-level thermocouple signals and magnetic signals (Hall probe voltages and pick-up coil voltage) need thus be amplified before acquisition. In addition, filtering is needed since we can no longer rely on measuring devices to reject either noise or normal-mode interference. The necessary signal conditioning is described below.

4.1 SIGNAL AMPLIFICATION

All signals coming from the instrumented sample are amplified with a home-made amplification card based on AD623 instrumentation amplifiers. These amplifiers are characterized by both a high input impedance and high common-mode rejection ratio. They are well suited to low-level (DC) thermocouple signals and low-frequency AC signals. The gain of the amplifier is fixed through an external resistor and is chosen to be equal to 101 for all channels.

In the presence of large AC magnetic fields, it is of prime importance to minimize inductive pick-up by twisting wires finely together. Although this was implemented with great care, an unwanted parasitic AC signal (superimposed to the useful input signal) remains. The amplification parasitic signal by the AD623 component may lead to a saturation of the input of the analog-to-digital converter (ADC). This is especially the case when, for the highest possible accuracy, the range of the ADC is set as close as possible to the expected voltage range of the useful signal. In order to avoid saturation of the ADC channels due to the unwanted AC voltage, a low-pass filter analog circuit is placed between the amplifier and the analog-to-digital converter.

Simultaneous magnetic and thermal measurements on our instrumented superconducting sample involves three kinds of signals: (i) thermocouples voltages, that can be considered as quasi-DC signals, (ii) the voltage across the pick-up coils, i.e. mainly an AC signal at the same frequency as the applied field, and (iii) the voltages across the Hall probes, containing an AC component possibly superimposed to a DC component when the superconductor is either magnetized permanently or subjected to a DC field superimposed to the AC field. Note also that both the pick-up coil and the Hall probe voltages may also contain harmonics due to the non-linear response of the superconductor. The characteristics of the signals are summarized in Table 1. The frequency of parasitic signals was determined experimentally from a fast Tourier Transform (FFT) of the amplified signals using a TDS 2024B Tektronix oscilloscope.

Signal	Type of useful signal	Frequency of main parasitic signals	Frequency cut-off
Thermocouples	**DC**	50 Hz, f , HF noise	30 Hz
Pick-up coil	**AC** (f + harmonics)	50 Hz, HF noise	50 kHz
Hall probes	**DC** + **AC** (f + harmonics)	50 Hz, HF noise	50 kHz

Table 1. characteristics of the signals coming from the instrumented sample subjected to an AC magnetic field of frequency f (experimentally between 56 and 108 Hz). The last column shows the cut-off frequency of the lowpass analog filter inserted between the instrumentation amplifier and the analog-to-digital converter.

A low-pass analog filter (Butterworth type, 2^{nd} order) is used for attenuating the parasitic signals. The cut-off frequency is set either at 30 Hz (for thermocouple signals) or at 50 kHz (for magnetic signals). Note that a notch filter at 50 Hz cannot be used in order avoid any signal distortion or phase-lag introduced by the filter. After realisation of the filter, we have checked experimentally that the phase-lag introduced by the 50 kHz filter is less than 1° for a 56 Hz input frequency and all its harmonics up to the 9^{th} (f = 504 Hz).

After amplification, analog filtering and sampling by the data acquisition card, some numerical treatment on the digitized signal is needed. For the (quasi-) DC signals from the thermocouples, the purpose is to remove remaining spurious AC voltages that are still superimposed on the useful signal. For the Hall probe signals, the aim is to extract the RMS and the DC components from the waveform. For the pick-up signal, the aim is to separate the in-phase and out-of-phase components of the AC signal, as a lock-in amplifier does.

4.2 DIGITAL AVERAGING

In the case of DC signals, all parasitic AC components have to be removed by an appropriate averaging procedure. Two kinds of interference signals affect the useful voltage: those at the power frequency (50 Hz) and those at the frequency f of the AC magnetic field (in our experiments, f ranges between 50 and 120 Hz). In order to average out both kind of signals to zero, the period of integration should be an integer multiple of the periods of both signals, i.e. 20 ms and (1/f). In practice, an integration time of 1 second was found to provide an excellent rejection of the AC parasitic signals in our case. In most applications, the corresponding sampling rate (1S/s) is high enough record the time-dependence of the temperature distribution. In the case of relatively "fast" temperature variations (typically $dT/dt > 5$ K /min) the integration time is sometimes reduced to 0.2 s in order to increase the sampling rate.

5. RESULTS

In this section, we report an experimental study of the self-heating behaviour of a bulk superconductor subjected to an AC magnetic field with the experimental system described.
The superconducting materials were synthesised by employing a TMSTG process described elsewhere (Hari Babu, 2006). The sample is a cylindrical large $YBa_2Cu_3O_7$ single domain pellet of diameter 30 mm and thickness 12 mm. Its superconducting transition temperature is $T_c \sim 91.6$ K.

The procedure used in the experiment is as follows. First the sample is cooled down to the liquid nitrogen temperature (77.4 K) in the absence of magnetic field. Next an AC magnetic sollicitation is applied and the magnetic properties of the samples and the temperature are recorded simultaneously. As an example, we study here the case where the AC magnetic field has an amplitude of 34 mT at $f = 91$ Hz. With such experimental conditions, one can show (Vanderbemden, 2010) that the sample temperature is expected to reach an equilibrium temperature close to the critical temperature in a short time, typically a few minutes. Due to such a fast temperature rise, we use the high-speed data acquisition system described above. The time-dependence of the temperature measured against the sample top surface by three thermocouples is plotted in Figure 4. Results are compared for the temperature at the centre ($r,z = 0,H/2$; red curve), at the edge ($r,z = R,H/2$, blue curve) and between these two locations ($r,z = R/2,H/2$, black curve). Qualitatively, the average temperature agrees nicely with the $T(t)$ behaviour predicted from our theoretical model (Vanderbemden, 2010).

The inset in Fig. 4 shows an enlargement of the graph during the first instants of the self-heating phenomena. The temperature are shown to raise first at the sample edge where losses are maximum. During the self-heating process, the maximum temperature difference measured on the top surface is ~ 0.1 K. Note the temperature increase starts as soon as the AC field is applied. Here the importance of thermal sensors characterised by a small response time is demonstrated.

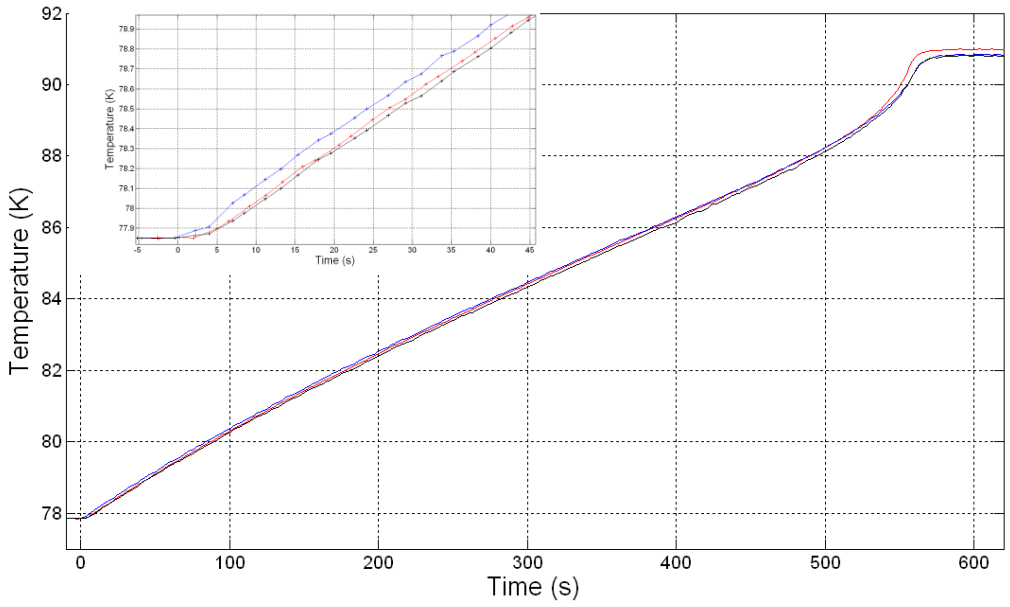

Figure 4. Time-dependence of temperatures at the surface of the superconducting sample during the application of a large AC magnetic field ($\mu_0 H_0$ = 34 mT – f = 91 Hz). The temperature measured by three thermocouples is shown in red for the centre position (r,z = 0,H/2), in blue for the edge position ($r \sim R$) and in black between those two locations (r = R/2). Inset: enlargement of the graph during the first instants of the self-heating phenomena.

The temperature dependence of the local AC magnetic induction probed by Hall sensors placed against the bottom face of the sample is shown in Figure 5, both for the centre position (r,z = 0,-H/2; red curve) and for the edge position (r,z = R,-H/2; blue curve). As the temperature of the superconductor increases, both the flux density measured at the centre B_C and near the edge B_E are found to increase monotonically, indicating a progressive reduction of the shielding properties of the superconductor. When the superconductor temperature is stabilized at the equilibrium temperature, both local inductions equal the applied magnetic induction within the resolution of our measurement, i.e. $B_E \approx B_C \approx \mu_0.H_0/\sqrt{2}$ as if the superconductor were in the normal state. In this regime however, the voltage across the pick-up coils of the susceptometer (not shown on the graph) differs from zero. This underlines that some parts of the superconductor – even close to its critical temperature T_c – remain in the superconducting (mixed) state; the thermal equilibrium results from the equality between the heat flux leaving the sample and the magnetic losses.

The thermal and magnetic data displayed in Figures 4 and 5 underline that superconductors, although characterized by a zero resistance, may exhibit significant losses when they are subjected to an AC magnetic field, however small. The losses induce a considerable self-heating leading to the apparent disappearance of the superconducting state, i.e. the final sample temperature is around its superconducting transition temperature.

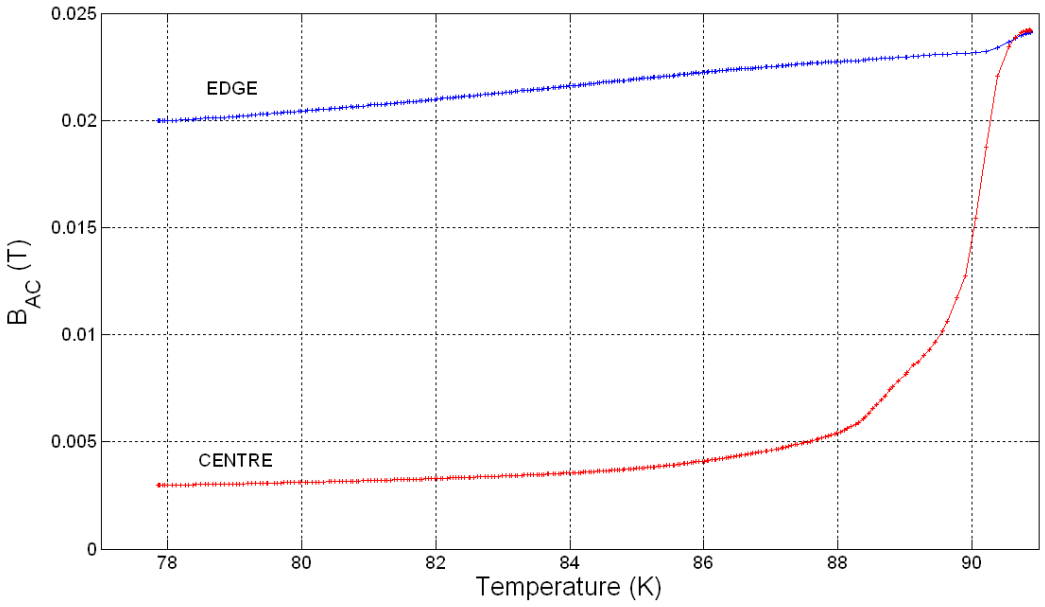

Figure 5. AC part of magnetic flux induction picked up by Hall sensors placed against the bottom surface of the bulk superconducting sample subjected to a 34 mT, 91 Hz AC magnetic field. The red and blue curves refer to the magnetic flux measured at the centre ($r = 0$) or near the edge ($r = R$) respectively. The data are plotted as a function of the average superconductor temperature.

6. CONCLUSIONS

We have successfully built and tested an experimental set-up for measuring the self-heating of a bulk superconductors subjected to a large AC magnetic field, possibly superimposed onto a DC magnetic field. In such an experiment, the main issue is to reduce the source of heat losses that may have a detrimental impact on the temperature measurement. In addition our system is able to measure simultaneously the magnetic properties of the superconductor.

We have first described the experimental precautions to be taken with cryogenic temperature measurement with thermocouples attached to the sample. In particular, the reference ("cold") junctions of the thermocouples are encapsulated in a bespoke system consisting of two alumina plates in order to improve the temperature stability. We have also determined that the control current in the Hall probes should ideally be less than 10% of the nominal value in order to limit the heat generation in the vicinity of the sample.

In our system, AC and DC magnetic fields are generated by two separate concentric copper coils, both immersed in liquid nitrogen. Unlike magnets that are designed for measuring magnetic properties at 77.4 K, i.e. when the sample is immersed in liquid nitrogen as well, a practical current limitation arises since the Joule effect caused AC current should not induce any perceptible temperature rise in the superconductor placed in the sample chamber. The source of frequency limitations, in particular because of the capacitive coupling between primary and secondary coil of the susceptometer, were reported and discussed. Our system is able generate AC magnetic fields up to 60 mT [RMS] in the frequency range 50-120 Hz, over a cylindrical volume of 32 mm diameter and 12mm height. The DC field that can be

superimposed to an AC field is limited to 160 mT, because of (i) the magnetic coupling between AC and DC coils and (ii) the necessity of limiting the coil temperature below ~ 92 K, i.e. the temperature at which a thermal runaway is likely to occur.

Finally, we have described a high-speed data acquisition system that can be used for recording temperature and magnetic data when the superconductor is subjected to large AC magnetic fields, i.e. when the temperature rises quickly and measurements need to be carried out at a high sampling rate. We have described the analog and digital conditioning system required for extracting low level signals in a noisy environment, in particular because of the large e.m.f. arising from inductive pick-up of the large AC magnetic fields by the measurement wires.

Our system was tested on a cylindrical bulk $YBa_2Cu_3O_7$ sample intended, e.g. for levitation purposes. It was shown that a relatively modest AC magnetic field (34 mT, 91 Hz) can lead to a fast temperature rise that was measured by the temperature sensors attached to the top surface of the sample. Such a temperature increase arising in bulk high temperature superconductors subjected to time-varying magnetic fields may thus alter appreciably their behaviour in practical applications. The apparatus developed in this work is expected to be helpful in characterizing and optimising the behaviour of bulk single domain superconductors in engineering applications.

ACKNOWLEDGMENTS

We thank D.A. Cardwell and N. Hari Babu for providing high quality bulk superconducting samples used in this study. We acknowledge M. Ausloos and B. Vanderheyden for fruitful discussions. The technical help of P. Harmeling and J. Simon has been greatly appreciated. We also thank the FNRS (CR.CH. 09-10 1.5.212.10), the ULg (ARC 11/16-03) and the Royal Military Academy of Belgium (F07/03) for cryofluid and equipment grants.

REFERENCES

Brentari, E. G. & Smith, R. V. (1958). Nucleate and film pool boiling design correlations for 0_2, N_2, H_2 and He. *Adv. Cryog. Eng.* 10, 325-341.

Campbell, A. M. & Cardwell, D. A. (1997). Bulk high-temperature superconductors for magnet applications. Cryogenics 37, 567-575.

Goldfarb, R. B., Lelental, M. & Thompson, C. A. (1991). Alternating-field susceptometry and magnetic susceptibility of superconductors in Hein R. A., Francavilla T. L. and Liebenberg D. H. (Eds.) *Magnetic susceptibility of superconductors and other spin systems* (pp. 49-80), New York : Plenum.

Fujishiro, H., Kawachi, M., Kaneyama, M., Fujiwara, A., Tateiwa, T., & Oka, T. (2006). Heat propagation analysis in HTSC bulks during pulse field magnetization. *Supercond. Sci. Technol.* 19, 540-544.

Gömöry, F., Lobotka, P. & Fröhlich, K. (1994). Variable temperature insert for a.c. susceptibility measurements at a.c. field amplitudes up to 0.1 T. *Cryogenics* 34, 837-838.

Gömöry, F. (1997). Characterization of high-temperature superconductors by AC susceptibility measurements. *Supercond. Sci. Technol*. 10 523-542.

Hari Babu, N., Iida, K., Shi, Y. & Cardwell, D. A. (2006). Processing of high performance (LRE)-Ba–Cu–O large, single-grain bulk superconductors in air. *Physica C* 445-448, 286-290.

Laurent, P., Fagnard, J. F., Vanderheyden, B., Hari Babu, N., Cardwell, D. A., Ausloos, M., & Vanderbemden, P. (2008). An ac susceptometer for the characterization of large, bulk superconducting samples. *Meas. Sci. and Technol*. 19, 085705.

Lousberg, G. P., Fagnard, J. F., Noudem, J. G., Ausloos, M., Vanderheyden, B., & Vanderbemden, P. (2009). Measurement of the magnetic field inside the holes of a drilled bulk high-Tc superconductor. *Supercond. Sci. Technol*. 22, 045009.

Nikolo, M. (1995). Superconductivity: a guide to alternating current susceptibility measurements and alternating current susceptometer design. *Am. J. Phys.* 63, 57-65, 1995.

Sundqvist, B. (1992). Thermal diffusivity and thermal conductivity of chromel, alumel and constantan in the range 100-450 K. *J. Appl. Phys*. 72, 539-545.

Trojanowski, S. & Ciszek, M. (2007). Race-track coils for measurements of AC energy losses in high temperature superconducting tapes. *Prz. Elektrotech*. 83, 26.

Vanderbemden, P. (1998). Design of an AC susceptometer based on a cryocooler. *Cryogenics* 38, 839-842.

Vanderbemden, P., Laurent, P., Fagnard, J. F., Ausloos, M., Hari Babu, N., & Cardwell, D.A. (2010). Magneto-thermal phenomena in bulk high temperature superconductors subjected to applied AC magnetic fields. *Supercond. Sci. Technol*. 23, 075006.

Yamaguchi, K., Ogawa, J., Sekizawa, S., & Tsukamoto, O. (2006). Measurement methods of AC losses in HTS bulk. *Physica C* 445-448, 395-398.

Zushi, Y., Asaba, I., Ogawa, J., Yamagishi, K., Tsukamoto, O., Murakami, M., & Tomita, M. (2004). Study of suppression of decay of trapped magnetic field in HTS bulk subject to AC magnetic field. *Physica C* 412-414, 708-713.